

Collapse of an *AB* copolymer single chain with alternating blocks of different stiffness

I. V. Neratova,^a P. V. Komarov,^{a,b*} A. S. Pavlov,^a and V. A. Ivanov^c

^aTver State University,
33 ul. Zhelyabova, 170002 Tver, Russian Federation.
Fax: +7 (482 2) 32 1274.

^bInstitute of Organoelement Compounds, Russian Academy of Sciences,
28 ul. Vavilova, 119991 Moscow, Russian Federation.
Fax: +7 (495) 135 6549 E-mail: pv_komarov@mail.ru

^cM. V. Lomonosov Moscow State University, Department of Physics,
1 Leninskie Gory, 119991 Moscow, Russian Federation.
Fax: +7 (495) 939 2988

Using the Langevin dynamics, we studied the conformational properties of an *AB* copolymer single chain built of alternating stiff and flexible blocks having different steady-state affinities to a solvent. Two opposite conditions were simulated, *viz.*, where a solvent is poor for stiff blocks and good for flexible blocks and *vice versa*. The behavior of the molecules built of equal-length blocks and long stiff blocks linked through short flexible junctions were considered. Upon transition of a chain to the compact state, nanostructures with different morphologies, such as bunches, networks, and others, can form.

Key words: block copolymer, the Langevin dynamics, poor/good solvent, nanostructures.

It is known that the behavior of a single polymer chain depends on properties of the medium.^{1,2} In a good solvent, the conformation of a macromolecule is defined by the interunit repulsion forces (since the solvent molecules aggregate on them), which results in the general chain swelling. Conversely, compact structures form if a polymer is in a poor solvent. This is due to the predominance of attractive forces, since monomers tend to minimize the solvent–contact area. During compaction, a polymer chain can undergo various conformational transitions depending on the degree of stiffness of its segments and their chemical composition. This is most pronounced in the case of biological macromolecules, such as proteins that (under certain conditions) can spontaneously form the secondary and tertiary structures.³ The use of such mechanisms of primary self-assembly is attractive in designing novel building blocks for nanostructured materials. A non-uniform distribution of stiffness is one of the possible factors influencing directly the geometry of linear macromolecules. Therefore, the investigation of the role of local stiffness in self-organization of a single macromolecule is topical.

In recent years, the behavior of homopolymeric systems have been thoroughly studied by different complementary theoretical methods,^{4–7} computer simulation, and other methods.^{8–20} Consideration of the dynamics

and kinetics of the collapse of a single polymeric chain has allowed establishing some general regularities of this process. For example, the coil–globule type transition in flexible chains is accompanied by the formation of the quasi-globular regions linked through unfolded blocks followed by their fusion into the compact globular state.⁸ To assess the conformational behavior of a single flexible homopolymeric chain, it should be noted that with a decrease in temperature, sufficiently long chains undergo transition to the state of "solid" (crystalline) globule; moreover, this state is observed in both the lattice and continuity models.^{21,22} As contrasted to the flexible polymers with the two-stage collapse,^{4,5,9,11} condensation of semiflexible and stiff chains occurs *via* a cascade of different equilibrium states. The behavior of semiflexible polymeric chains in poor solvents have been studied^{12–14} by Brownian dynamics. It was proved that there exists a common pathway of the collapse of such systems, which passes through the stage of "long-lived" partially collapsed states, *e.g.*, the "racquet" conformation during the formation of torus. The energy parameters for two possible collapse pathways, *viz.*, direct formation of the toroidal structure and its formation through highly ordered structures, were compared.¹²

When studying the condensed states, a semi-flexible copolymer comprising monomers of two types having different affinity to a solvent were considered and a wide

variety of metastable structures, such as figure-eight structure, structures of a two-fold torus, and "tennis-racquet" were found.¹⁵ The resulting figure-eight structure was the most stable. It was shown¹⁶ that, if the chain stiffness is alternating, the semiflexible polymers with amphiphilic monomeric units can form cylindrical, collagen-like, and toroidal structures, two latter configurations have approximately equal energies.

Semiflexible polymers can be structured as various liquid crystal phases. The variety of the conformational behavior of these systems depends directly on the chain stiffness and temperature.^{7,9,10,17–19} The phase diagrams has been plotted for a semiflexible chain, which showed that the transitions resulting in the formation of intramolecular liquid crystal states can occur, where the compact globular state can be orientationally ordered not only in the conformation of toroid or cylindrical globule, but also in the conformation of virtually spherical globule.¹⁷

The description of the conformational properties and phase transitions of inhomogeneous molecules requires the detailed study, finding the regularities and features of their behavior, which stimulates interest in such objects in the modern polymer science. Inhomogeneous systems are characterized by a more complex and dissimilar behavior compared to homogeneous polymers. The macromolecule of the *AB* copolymer consisting of units of two types grouped into blocks *A* and *B* is one of the heteropolymer chain types, where said blocks can differ in both the internal characteristics, such as intrachain stiffness, and external characteristics, such as affinity to a solvent and adsorption properties with regard to the surfaces present in the system. Many research teams have performed studies of the conformational behavior of the *AB* copolymers consisting of flexible blocks with different affinities to the solvent. Particularly, the dependence of the formation of various globular morphologies on the primary sequence of the *A* and *B* units in a macromolecule has been studied in detail (e.g., see reviews^{23,24}). The simultaneous presence of flexible and stiff segments in one chain allows one to assume that the behavior of such systems will be non-trivial compared to homopolymers. The behavior of a single chain of a regular polymer comprising two types of equal-length blocks has been studied by Brownian dynamics.²⁰ It was shown that the change in the stiffness of chain segments with a length of 200 monomers leads to the change in the molecule ordering due to the collapse in the case where a solvent is poor for monomers of one defined type, which is accompanied by the formation of bunches and network structures.

The aim of the present work is to study the collapse of the polymers comprising blocks of different stiffness. A regular *AB* copolymer with alternating flexible and stiff blocks is the simplest example of such systems. A protein macromolecule with the secondary-structure regions of

different stiffness (α -helices and flexible junctions) can serve as the real analog of such chains.

In contrast to the model studied earlier,²⁰ we decided to study the influence of the overall chain length *N* and the length of blocks *A* and *B* on the conformational steady-state behavior of a single polymeric chain. The macromolecule is assumed to be in a selective solvent. In particular, we consider the cases where a solvent is poor (in terms of thermodynamics) for stiff fragments and good for flexible fragments and *vice versa*. Such selectivity of a solvent causes the formation of multiform structures of a single chain, which will be described below.

Model

The copolymer molecule was represented as a linear sequence of *N* spherical particles, *viz.*, the beads of two types *A* and *B* with the diameter $\sigma = 1$, linked through the fixed-length stiff bonds (Fig. 1). The type *A* beads form stiff blocks, whereas those of type *B* form flexible blocks, which consist of n_s and n_f particles, respectively. The numbers of flexible and stiff blocks were regulated by the parameters N_A and N_B , the $N_A : N_B$ ratio being equal to 1 : 1 in all computations. Taking into account the introduced parameters, the overall chain length (*N*) is $N = N_A n_s + N_B n_f$. Note that, when setting the model parameters, we used the standard reduced units, *i.e.*, the length unit was σ , the energy unit was ϵ , the time unit was $\tau = (m\sigma^2/\epsilon)^{1/2}$, where *m* is a weight, and the temperature unit was $T = \epsilon/k_B$, where k_B is Boltzmann's constant. The values of force

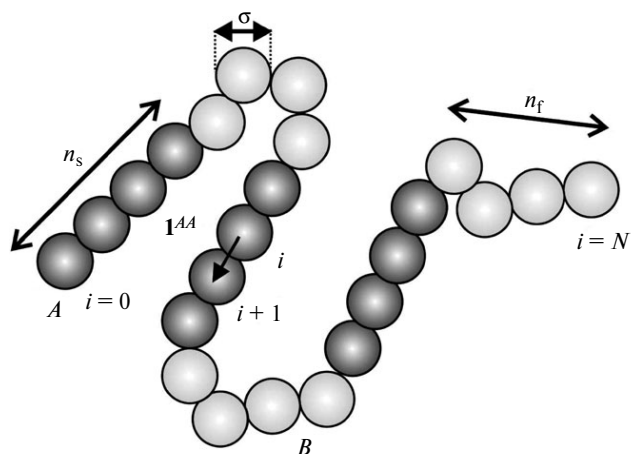


Fig. 1. The model and main parameters of a polymeric chain: n_s and n_f are lengths of stiff and flexible blocks, respectively; *N* is the overall chain length; σ is a diameter of particles forming a chain; \mathbf{l}_i^{AA} is an example of setting the unit vector between the particles with the numbers *i* and *i* + 1, which is used for calculation of the order parameter for stiff blocks. Here and in Figs 4 and 6–8, the stiff blocks (type *A* beads) of a chain are shown in dark color, whereas the flexible ones (type *B* beads) are shown in light color.

constant (ϵ) and weight (m) were taken equal to unity in all computations.

The polymer chain stiffness was regulated by three harmonic potentials:

$$\begin{aligned}
 U_{\alpha}^{(\text{angle},1)}(r_1, r_{i+1}, r_{i+2}) &= \frac{1}{2} k_{\alpha}^{\text{angle},1} (\varphi - \pi)^2, \\
 \varphi &= \arccos \left(\frac{\mathbf{r}_{i+1,i} \cdot \mathbf{r}_{i+1,i+2}}{|\mathbf{r}_{i+1,i}| |\mathbf{r}_{i+1,i+2}|} \right), \\
 U_{\alpha}^{(\text{angle},2)}(r_1, r_{i+2}, r_{i+4}) &= \frac{1}{2} k_{\alpha}^{\text{angle},2} (\theta - \pi)^2, \\
 \theta &= \arccos \left(\frac{\mathbf{r}_{i+2,i} \cdot \mathbf{r}_{i+2,i+4}}{|\mathbf{r}_{i+2,i}| |\mathbf{r}_{i+2,i+4}|} \right), \\
 U_{\alpha}^{(\text{angle},3)}(r_1, r_{i+3}, r_{i+6}) &= \frac{1}{2} k_{\alpha}^{\text{angle},3} (\psi - \pi)^2, \\
 \psi &= \arccos \left(\frac{\mathbf{r}_{i+3,i} \cdot \mathbf{r}_{i+3,i+6}}{|\mathbf{r}_{i+3,i}| |\mathbf{r}_{i+3,i+6}|} \right),
 \end{aligned} \quad (1)$$

where $\alpha = \{AA, AB, BB\}$. The potential constants are related as follows: $k_{\alpha}^{\text{angle},2} = k_{\alpha}^{\text{angle},1}/2$, $k_{\alpha}^{\text{angle},3} = k_{\alpha}^{\text{angle},2}/2$. Determination of the angles φ , θ , and ψ is shown in Fig. 2. Introduction of additional potentials to the bond angle strain potential $U_{\alpha}^{(\text{angle},1)}$, namely, through two ($U_{\alpha}^{(\text{angle},2)}$) or three ($U_{\alpha}^{(\text{angle},3)}$) beads provides a high polymer chain stiffness and allows no decreasing the integration step of equations of motion. The parameters of the potential $U_{\alpha}^{(\text{angle},i)}$ for stiff and flexible blocks were determined from the analysis of the properties of the polymeric

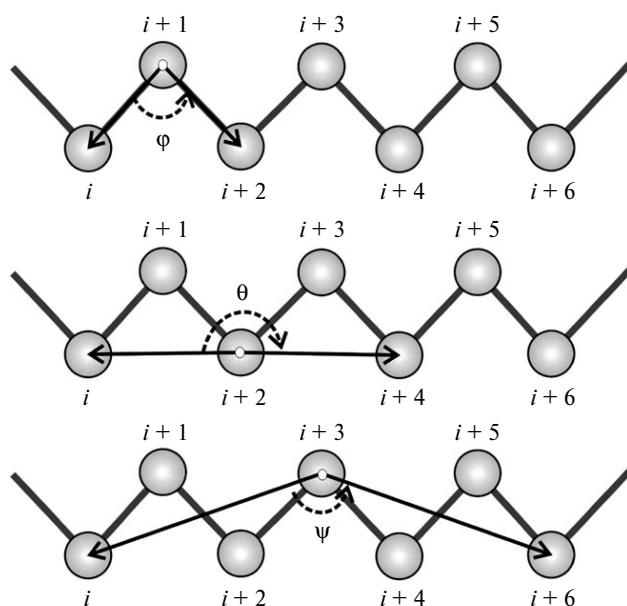


Fig. 2. Determination of the angles φ , θ , and ψ , which are necessary for calculation of the three-particle potentials (1), here $\mathbf{l}_i \equiv \mathbf{r}_{i+1} - \mathbf{r}_i$, $|\mathbf{r}_{i+1} - \mathbf{r}_i| = \sigma$.

chain ($N = 1260$, $n_s = n_f = 9, 15, 30$) in the case where a solvent is simultaneously good for all blocks. The selected value for $k_{AA}^{\text{angle},1} = 25 \epsilon \text{ rad}^{-2}$ allows the length of the Kuhn segment l_K of a stiff block to be approximately equal to the length of the block itself (i.e., $l_K \approx n_s \sigma$). In the case of flexible blocks, $k_{BB}^{\text{angle},1}$ is equal to 0, which results in $l_K \approx \sigma$. Since the stiffness is regulated only between the beads of one type, the force constant $k_{AB}^{\text{angle},1}$ is equal to zero.

The non-bonded interactions of the chain beads are described by the potential

$$\begin{aligned}
 \begin{cases} U_{\alpha}(r_{ij}) = U_{\alpha}^{(LJ)}(r_{ij}) - U_{\alpha}^{(LJ)}(r_{\text{cut}}^{(\alpha)}), & \forall r_{ij} \leq r_{\text{cut}}^{(\alpha)}, \\ U_{\alpha}(r_{ij}) = 0, & \forall r_{ij} > r_{\text{cut}}^{(\alpha)}, \end{cases} \\
 U_{\alpha}^{(LJ)}(r_{ij}) = 4\epsilon_{\alpha} \left[\left(\frac{\sigma}{r_{ij}} \right)^{12} - \left(\frac{\sigma}{r_{ij}} \right)^6 \right],
 \end{aligned} \quad (2)$$

where $U_{\alpha}^{(LJ)}$ is the Lennard-Jones potential, $\alpha = \{AA, AB, BB\}$, ϵ_{α} is an energy parameter ($\epsilon_{\alpha} = 1\epsilon$), r_{ij} is the distance between the particles i and j ($i \neq j$), and $r_{\text{cut}}^{(\alpha)}$ is a potential cutoff radius. It is assumed that the beads of different types (A and B) interact with each other through steric repulsion. Therefore, in the case when $\alpha = AB$, the value for $r_{\text{cut}}^{(AB)}$ was selected to be equal to $2^{1/6}\sigma$. In other two cases where $\alpha = AA, BB$, the parameter $r_{\text{cut}}^{(\alpha)}$ was used for switching the modes of poor and good solvents. Let us consider this case in more details.

To date, the concept of poor and good solvents has become commonplace when characterizing solutions of homopolymer macromolecules.^{1,25} A solvent is considered as good, if the force of its interaction with a polymer is greater than the force of interaction between the polymeric chain units. In this case, macromolecules acquire the shape of a swollen coil and the free solvent volume becomes minimal. The condition of a good solvent was set by introduction of the potential cutoff radius $r_{\text{cut}}^{(\alpha)}$ equal to $2^{1/6}\sigma$. With this $r_{\text{cut}}^{(\alpha)}$ value, the beads of a model chain can interact with each other only through the repulsive part of the potential (2). This means that the monomers of a polymeric chain are completely surrounded by the solvent molecules shielding their interaction.

The poor solvent is characterized by that the force of interaction of polymeric units between themselves is greater than the force of interaction of a polymer with the solvent. For this reason, the polymeric chain tends to minimize the solvent-contact surface and passes to a compact globular conformation. The volume ratio of a solvent in a globule decreases (if its chain is sufficiently flexible), as a result of which the free solvent molecules fill the space between the collapsed polymeric chains. In the model under consideration, the condition of a poor solvent was introduced by setting the value of $r_{\text{cut}}^{(\alpha)}$ equal to $4 \cdot 2^{1/6}\sigma$. At such a radius of the potential action, its attractive part is

"involved", which allows the beads to be attracted to one another. Note that this selection of the cutoff radius is caused by the considerations of computational cost minimization.

In addition, it must be emphasized that the conditions of good and poor solvents are also regulated by the values of the force constant ε_a of the potential (2). According to Flori,²⁵ a certain temperature θ exists for each specific value of the energy parameter ε_α . The repulsive forces predominate between the chain units interacting through the potential (2) at high temperatures when $T > \theta$, whereas the attractive forces predominate at low temperatures ($T < \theta$). Determination of the θ points for $\varepsilon_\alpha = 1\varepsilon$ and $r_{\text{cut}}^{(\alpha)} = 4 \cdot 2^{1/6} \sigma$ ($\alpha = AA, BB$) was performed for the chain consisting of $N = 1260$ beads (within the framework of the model under consideration) and the length of a flexible and a stiff block was selected to be equal, $n_s = n_f = 15$. Instead of the θ point, we determined, in fact, the coil–globule type transition temperature by the position of the inflexion point of the function $\langle r_{1N}^2 \rangle(T)$ expressing the temperature dependence of the mean squared distance between the chain ends. However, as is well known,²⁵ both these temperatures coincide at the limit of infinitely long chain; therefore, we will speak about the θ point hereinafter for the sake of simplicity. For selected values of ε_α and $r_{\text{cut}}^{(\alpha)}$, we obtained the value $\theta = 2\varepsilon/k_B$ for the temperature θ . Thereby, we obtained the value for the temperature θ for the case where both blocks have the attraction potential between the beads, but, as before, only the repulsion potential acts between the beads of different blocks due to the excluded volume. For the case studied in this work, where attraction acts only between the beads of one type blocks, in view of the variety of emerging metastable structures, the problem of obtaining the temperature θ is non-trivial and falls beyond the scope of the present work. The temperature $T = 1\varepsilon/k_B$ selected for simulation provided the collapse of a copolymeric chain in all systems studied.

The study of the collapse of an *AB* copolymer single chain at the constant temperature $T = 1\varepsilon/k_B$ ($T < \theta$) was performed within the framework of the Langevin dynamics.^{26,27} The system evolution is described by solution of the simultaneous stochastic equations of motion written in the form of the Langevin equations

$$m_i \ddot{\mathbf{r}}_i = -\frac{\partial}{\partial \mathbf{r}_i} U - \sum_{\alpha=1}^{N-1} \lambda_\alpha \frac{\partial}{\partial \mathbf{r}_i} f_\alpha - m_i k \dot{\mathbf{r}}_i + \mathbf{F}_i^{(C)}, \quad (3)$$

$$i = 1, \dots, N$$

with supplementary conditions

$$f_\alpha(t) = |\mathbf{r}_\alpha(t) - \mathbf{r}_{\alpha+1}(t)| - \sigma = 0, \alpha = 1, \dots, N-1,$$

where m_i is a weight of the i -th bead ($m_i \equiv m$), \mathbf{r}_i is the radius vector, λ_α are the undetermined Lagrangian multipliers, k is a friction coefficient. The value $k = 0.5\tau^{-1}$ was selected as a compromise, wherein the mean temperature is maintained with acceptable accuracy ($\langle T \rangle =$

$= 1.00038 \pm 0.02777 \varepsilon/k_B$) and the beads have sufficient mobility. The summands included in the right part of equation (3) describe, respectively, the forces acting on the i -th bead from the side of other particles, the reaction of stiff bonds, interaction with a solvent (viscous friction force), and the thermal reservoir $\mathbf{F}_i^{(C)}$ (stochastic Brownian force of thermal noise). In our model, the total potential energy U of a system is defined as a sum of all potentials of types (1) and (2) acting between the chain beads. The stochastic force is calculated as the time- δ -correlated Gaussian random process following the fluctuation–dissipation theorem.²⁸ Therefore, the first and second moments for $\mathbf{F}_i^{(C)}$ satisfy the following relations

$$\langle \mathbf{F}_i^{(C)}(t) \rangle = 0, \langle \mathbf{F}_i^{(C)}(t) \mathbf{F}_j^{(C)}(t + \tau) \rangle = 2m_i k_B T \delta_{ij} \delta(\tau),$$

where angular brackets designate time averaging, $\delta(\tau)$ is the delta function, δ_{ij} is the Kronecker delta. The presence of stochastic force converts all dynamic variables into the random ones.

To take integral of the set of equations (1), we used the standard "leap-frog" version of the Verlet algorithm²⁹ in combination with the Shake algorithm,³⁰ which performs the search for the undetermined Lagrangian multipliers λ_α and correction of the coordinates of the beads \mathbf{r}_i .

Each of the initial chain configurations was generated in a random manner on a cubic lattice (at σ intervals) by successive connection of monomers to the desired value N (chain self-crossings were excluded). Then relaxation of the chain obtained was performed under the conditions of a good solvent for the beads of all kinds. The integration step for the motion equations (3) Δt was set to be equal to 0.01τ , the accuracy for the convergence of iterative procedure in the Shake algorithm being 10^{-7} . The duration of the cycle of initial system conditioning for each set of parameters was about $3 \cdot 10^6$ integration steps Δt . The transition into the equilibrium state was determined by stabilization of the system potential energy U and the absence of the macromolecule size drift (mean-square distance between the chain ends) at sufficiently prolonged time intervals ($\sim 1 \cdot 10^6 \Delta t$). The equilibrium conformations of chains obtained as a result of the above-described procedure were used as starting for the study of their behavior upon change in the external conditions.

The duration of subsequent productive count t_{max} depending on the length of the chain under study was from $1 \cdot 10^6$ to $100 \cdot 10^6 \Delta t$. Since we were interested in the steady-state structural properties of collapsed chains (which we call as a final state), for its identification we performed the calculations of such characteristics as the energy of van der Waals interactions (E_{vdw})

$$E_{\text{vdw}} = \sum_{\alpha, j > 1} U_\alpha(r_{ij})$$

and the orientational order parameter S (for stiff blocks). The equilibrium state was considered to be achieved when

the curves $E_{\text{vdw}}(t)$ and $S(t)$ reach a plateau and the mean-square deviation of these values became less than 0.01. The order parameter S was determined as the maximum eigenvalue of the symmetric matrix with entries $S_{\tau\nu}$

$$S_{\tau\nu} = \frac{1}{2} \frac{1}{(N_A - 1)} \sum_{i=1}^{N-1} \left[3 \frac{l_{i,\tau}^{AA} \cdot l_{i,\nu}^{AA}}{(l_i^{AA})^2} - \delta_{\tau\nu} \right], \quad (4)$$

$\tau, \nu = \{x, y, z\},$

where $l_{i,\tau}^{AA}$ are projections of the vectors \mathbf{l}_i^{AA} ($l_i^{AA} = |\mathbf{l}_i^{AA}|$) connecting the beads i and $i + 1$ at the axis x, y, z (see Fig. 1); $\delta_{\tau\nu}$ is the Kronecker delta. For $S = 1$, all stiff fragments are collinear.

Results and Discussion

Based on the designed model, we studied the behavior of single chains of the regular *AB* copolymer upon changes in the external conditions, which were set by the quality of a solvent for stiff and flexible blocks. Two opposite cases were considered, *viz.*, that where stiff blocks of a chain (type *A* beads) are in a poor solvent and flexible blocks (type *B* beads) in a good solvent and *vice versa*. We have not been interested in the influence of the lengths of flexible and stiff blocks on the final state of a chain. To facilitate the analysis of the system behavior, the first stage of calculations was performed for the chains where the lengths of stiff and flexible blocks are equal, *i.e.*, $n_s = n_f \equiv n$. At the second stage, the length of a flexible block n_f did not change and was selected to be considerable shorter than the length of a stiff fragment (the case where flexible junctions are present in the chain). Depending on the variant of calculation, the overall chain length N varied from 360 to 2520 beads. The close model with the overall chain length $N = 200$ and the length of blocks $n = 10$ was considered;²⁰ however, in our view, ten stiff block are insufficient to make conclusion on the behavior of a polymeric macromolecule. It should be noted that prolonged stabilization of $E_{\text{vdw}}(t)$ and $S(t)$ in itself does not ensure the transition of a system into the most energetically favorable state; therefore, we performed five independent calculations from statistically independent states for each set of parameters as an additional check of the reproducibility of final states.

The study of the influence of the block length on the geometry of the final state of a polymeric chain in a selective solvent included three series of calculations. First, we considered the case where the condition of a poor solvent was fulfilled for stiff segments of a chain. As noted above, in this case, $n_s = n_f$ and $N_A : N_B = 1 : 1$. Simulation was performed for the molecules having the length of $N = 630$, 1260, and 2520 spherical particles. Such selection of the parameters N is caused by the convenience of the chain splitting in short blocks including $n = 9, 15, 21$, and

30 beads whose lengths are divisible by simple dividers 2, 3, 5, and 7.

Figure 3 shows an example of the collapse of the chain consisting of 630 beads with the length of stiff and flexible block $n = 21$ on the time interval $45 \cdot 10^6 \Delta t$. The configuration obtained by preliminary equilibration of a system under the conditions of a good solvent was used as the starting conformation ($t = 0$). The initial value $E_{\text{vdw}}(0)$ in Fig. 3 corresponds to the full van der Waals energy of a chain at the time of inclusion of the conditions of a poor solvent for stiff blocks (type *A* beads), the conditions of a solvent remaining for flexible blocks (type *B* beads). As can be seen from Fig. 3, the function $E_{\text{vdw}}(t)$ has a stepped form. Each step in the graph corresponds to the formation and enlargement of the clusters consisting of collapsed stiff blocks. The examples of snapshots of a system corresponding to different t are shown in Fig. 4. The horizontal region in the graph $E_{\text{vdw}}(t)$ for $t > 25 \cdot 10^6 \Delta t$ (see Fig. 3) corresponds to the final state of the system. In the case of this system, identification of the final state is unambiguous. The chain conformation in the region $t > 25 \cdot 10^6 \Delta t$ does not change and is well-reproducible tapered structure where stiff blocks are arranged in parallel to each other (see Fig. 4, *c*). Although this conformation is well reproduced starting from the statistically independent states, its full energy is not the lowest. Since the chain comprises flexible blocks extended in parallel to stiff blocks, the latter undergoes relative shifts, which decreases necessarily their ordering and, as a consequence, the full energy of the system. This is easily checked by a comparison of the values U for the obtained structures with the energy of prepared state of the chain where all stiff blocks have parallel packing and flexible blocks are concentrated near the flanking sides of the globule. However, the formation of

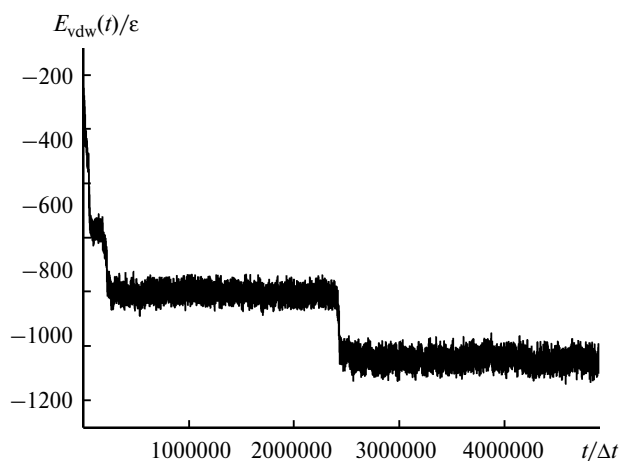


Fig. 3. The time dependence of the van der Waals interaction energy E_{vdw} for the chain of a regular *AB* copolymer ($n_s = n_f \equiv n$), $N = 630$, $n = 21$ at $T = 1\epsilon/k_B$. The conditions of a poor solvent are fulfilled for the stiff segments of a chain that are built of the type *A* beads.

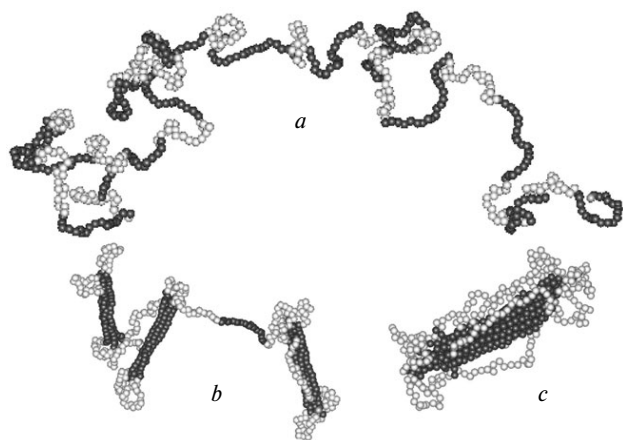


Fig. 4. The main steps of the collapse of an *AB* copolymer regular chain ($N = 630$, $n = 21$ at $T = 1\epsilon/k_B$): *a* is an initial relaxed state ($t = 0$), *b* is an intermediate state with several clusters ($t = 25000 \Delta t$), *c* is a collapsed chain ($t = 3 \cdot 10^6 \Delta t$). The conditions of a poor solvent are fulfilled for the stiff segments of a chain that are built of the type *A* beads ($n_s = n_f = n$).

such conformations distinguished by high ordering is unfavorable as regards entropy. Since several clusters of stiff blocks with a random relative orientation arise during the chain collapse, aggregates will be the most probable upon their subsequent coalescence, wherein the part of flexible blocks is extended along the collapsed stiff segments of the chain.

Upon changes in the parameters n and N , the behavior of the van der Waals energy is similar to the behavior of $E_{vdw}(t)$ in Fig. 3 and characterized by different number of stepped regions, their relative positions, and lengths. It should be noted here that the collapse time increases considerably as N increases; therefore, for long chains with $N \geq 2520$, it is problematic to obtain the equilibrium structures.

As noted above, to identify whether the system has achieved the equilibrium state and to characterize the final conformation, in addition to $E_{vdw}(t)$, we calculated the order parameter S according to equation (4). As in the case of $E_{vdw}(t)$, the behavior of the order parameter for the most of the chains under consideration has a higher degree of similarity. The examples of the behavior of $S(t)$ for different molecules are shown in Figs 5, *a* ($N = 630$, $n = 9, 15, 21$) and 5, *b* ($N = 630, 1260, 2520$, $n = 21$). One can observe two characteristic regions in the behavior of $S(t)$: slow growth accompanied by strong fluctuation of $S(t)$ by value and subsequent stabilization upon reaching the plateau. The growth of $S(t)$ suggests the formation of oriented structures in the subsystem of stiff blocks. The considerable fluctuations of the order parameter occur due to the simultaneous formation of several clusters on the chain whose orientation changes during relative motion (see Fig. 4, *b*). Such conformational behavior of chains

during collapse results in the emergence of deep holes and sharp peaks on the curve $S(t)$. During connection of several aggregates into a single globule, slow ordering of the orientations of particular clusters occurs; therefore, the curve $S(t)$ comes up to the horizontal region, which, for the most of systems, suggests the achievement of the equilibrium state. In this case, the horizontal region on the curve $S(t)$ corresponds to the analogous regions on the curve $E_{vdw}(t)$ (see Fig. 3 and Fig. 5, *a*, curve 3).

Figure 6 shows the examples of the snapshots of the collapsed states of the copolymer with $N = 630, 1260, 2520$ and the lengths of stiff and flexible blocks $n = 9, 15, 21, 30$, which arise most often in the series of five independent calculations. Each of the represented conformations corresponds to the saturation region on the curves $S(t)$ and $E_{vdw}(t)$. The stiff blocks with the lengths $n \geq 15$ form the

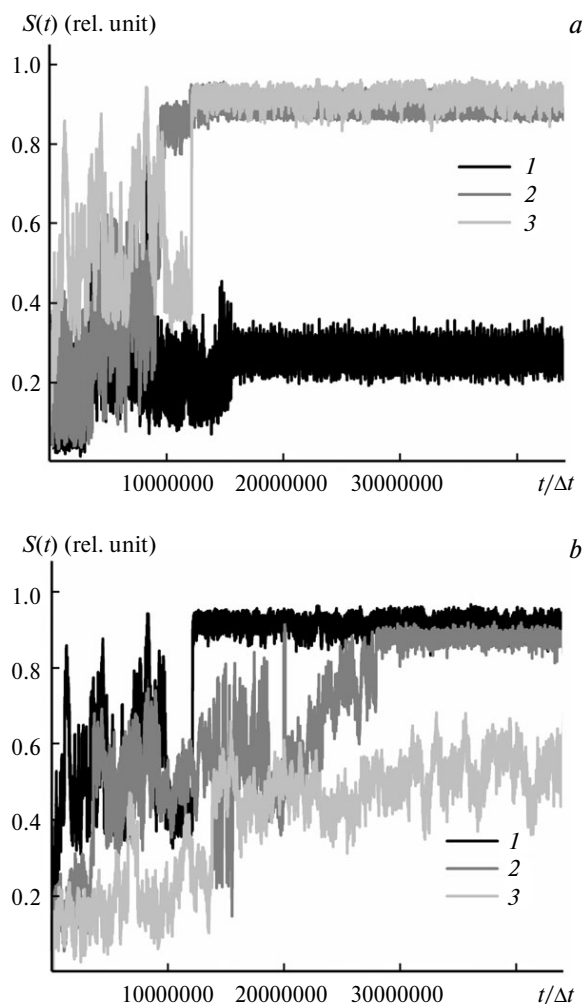


Fig. 5. The time dependence of the order parameter S during the collapse of an *AB* copolymer regular chain: *a* — $N = 630$, $n = 9$ (1), 15 (2), 21 (3), *b* — $n = 21$, $N = 630$ (1), 1260 (2), 2520 (3). The conditions of a poor solvent are fulfilled for the stiff segments of a chain that are built of the type *A* beads, $T = 1\epsilon/k_B$ ($n_s = n_f = n$).

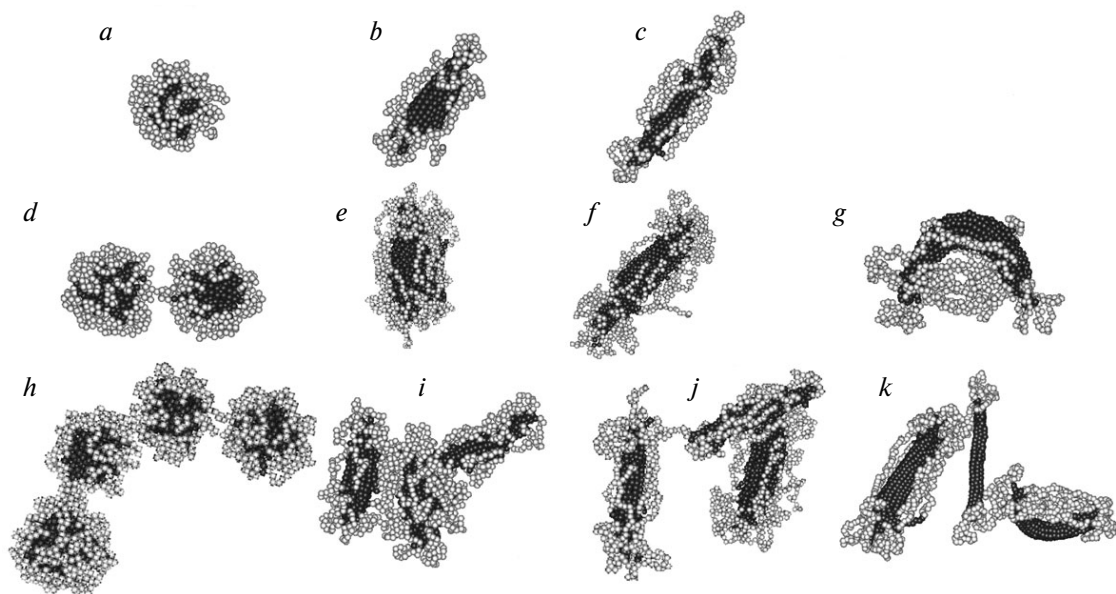


Fig. 6. Examples of the conformations of the collapsed chain of a regular *AB* copolymer at the time $t = 5 \cdot 10^6 \Delta t$ at $T = 1\epsilon/k_B$: $N = 630$, $n = 9$ (a), 15 (b), 21 (c); $N = 1260$, $n = 9$ (d), 15 (e), 21 (f), 30 (g); $N = 2520$, $n = 9$ (h), 15 (i), 21 (j), 30 (k). The case where $N = 630$, $n = 30$ was not considered, since, for this N under the condition $N_A : N_B = 1 : 1$, there is no integer number of the *A* and *B* blocks. The conditions of a poor solvent is fulfilled for the type *A* beads.

ordered parallel configurations in the form of bunches. When $N = 630$ at $n = 9, 15, 21$, and $N = 1260$ at $n = 15, 21, 30$, one globule forms (see Fig. 6). The conformations of the collapsed chain for $N = 630, 1260$ at $n = 15, 21$ are characterized by the maximum ordering for the subsystem of stiff blocks, which shows the mean value of the order parameter in the saturation region $\langle S \rangle \approx 0.7-0.9$ (see Fig. 5, a, curves 2, 3 and Fig. 5, b, curve 2). The shown examples of the behavior of the order parameter and the reproducibility of the final states allow one to state that the chain conformations given in Fig. 6 (a–c, e–g) are final.

The results of simulation demonstrate that, for all n , flexible junctions are partially extended along a globule. As discussed above, this occurs due to the coalescence of several clusters whose orientation relative to each other was random. In the case of long blocks ($n = 30$), this fact results in the inflexion of the globule that formed. As a result, a sickle-shaped structure with the mean order parameter of ~ 0.71 forms (see Fig. 6, g).

When the block length is short, e.g., $n = 9$ and $N = 630$, no parallel packing of stiff fragments was observed in the final state. The example of this conformation is shown in Fig. 6, a. For this system, the mean order parameter in the saturation region is $\langle S \rangle = 0.29$ (see Fig. 5, a, curve 1). As the number of blocks grows at their fixed length $n = 9$, i.e., upon increase in the overall chain length ($N = 1260$ and 2520), several globules connected through flexible junctions and covered with a hydrophilic edge form in the final state (see Fig. 6, d, h). The order parameter $\langle S \rangle$ for such

conformations is 0.20 and 0.25. The formation of several globules in the final states (as has been noted above) is associated with the mechanism of nucleation, as a result of which several active centers emerge simultaneously on the copolymer chain. Such behavior has been observed upon transition of the homopolymeric chain into the globular state where the necklace-like structure formed as an intermediate.^{31–33} However, owing to the formation of a hydrophilic edge, the hydrophobic blocks were isolated from the possible contact and, as a consequence, from subsequent coalescence into the compact structure. The presence of a hydrophilic edge prevents the formation of the compact tapered aggregates shown in Fig. 6, i–k in the case where $N = 2520$ at $n = 15, 21, 30$. The answer to the question whether the described conformations are stable or metastable is still open. On the time interval achieved ($10^8 \Delta t$), we did not observe noticeable changes in the detected chain states, which form during the first $10-30 \cdot 10^6$ steps Δt of a productive count. The example of the change in the order parameter for $N = 2560$ at $n = 21$ on the interval $45 \cdot 10^6 \Delta t$ is shown in Fig. 5, b (curve 3). On the time interval when $t > 15 \cdot 10^6 \Delta t$, the behavior of $S(t)$ is stabilized and fluctuates around the mean value ~ 0.54 . The calculation of different initial states showed that the necklace-like conformations are reproduced. The number of stiff blocks in the composition of particular aggregates varies greatly in the case where $n > 15$.

In the second series of calculation, the length of a flexible block n_f was not changed and was selected to be considerably shorter than the length of a stiff fragment

(the case where short flexible junctions are present in the chain). The values selected for simulation were as follows: $n_f = 3$ and $n_s = 9, 15, 21$, and 30 . Depending on the number and length of stiff blocks, the overall chain length was 378, 693, and 756 beads. The passage to the system with short flexible junctions results in the homotypic well-reproducible sheaf-like structure of a globule when using the series of statistically independent starting conditions on the time interval $50 \cdot 10^6 \Delta t$. Therefore, there is no doubt that all systems under consideration achieve the equilibrium state. The mean values of the order parameter in the saturation region varies in the range of $0.75\text{--}0.9$. All "hydrophilic" units are concentrated near the flanking surfaces of a globule and a small part of stiff fragments is folded in halves (Fig. 7, *a*). Such a structure forms due to the coalescence of several aggregates randomly distributed along the chain. The remaining loops contain the odd number of stiff fragments, which results in the inflexion of the bunch that is forming (Fig. 7, *b*). When falling into the globule core, a short hydrophilic block decreases slightly the attraction energy and, therefore, the globules that seem to consist of two parts spliced by the flanking surfaces are produced in this system (Fig. 7, *c*). The similar conformation was observed for the case where $N = 1260$ at $n_s = n_f = 15$ (see Fig. 6, *e*). For blocks with $n_s = 9$ in the case of short flexible junctions ($n_f = 3$), no orientational ordering in the globular state was detected.

In the third series of calculation, we studied the collapse of the model chain where the type *B* flexible fragments are under the conditions of a poor solvent. The parameter region as selected for the first and second series of calculations was studied. The examples of the states formed in the case $n_s = n_f$ are shown in Fig. 8. In almost all cases, the network structures where stiff blocks connected

through the nodes of the condensed polymer are produced as a result of the collapse. The presence of long stiff blocks between the network nodes does not allow them to come close and stabilizes the forming aggregate. The mean order parameter in the saturation region varies in the range of $0.19\text{--}0.24$. In the final state, there was a great variety of states whose morphologies depend on the starting conditions. However, by changing the length of blocks, one can control the size of forming grid cells (see Fig. 8). We assumed that the formation of network aggregates as a result of the collapse of polymer chains under the conditions of a semidilute solution can serve as a basis for design of novel membrane materials.

Thus, using the Langevin dynamics, we performed the study of equilibrium structural properties of the collapsed single chain of a regular *AB* copolymer consisting of blocks of different intrachain stiffness. Much attention was given to the influence of the change in the overall chain length and the length of its segments on the final state of a system by changing the external conditions, which were set by the quality of a solvent for blocks of different kind.

The obtained results evidence that, under the conditions of a poor solvent, the multiblock copolymer with flexible and stiff blocks of equal lengths can form reproducible secondary heterogeneous structures of two morphologies, *viz.*, a spheric globule and a bunch. In the case of short flexible junctions, the bunch-type conformation is the final state of the collapsed chain. The chain collapse under the conditions of a poor solvent for flexible blocks results in the formation of grid structures. The size of formed grid cells can be controlled by changing the length of copolymer chain blocks. The presence of orientational order in the final structures makes them potentially applicable in optical devices. The formation of networks with

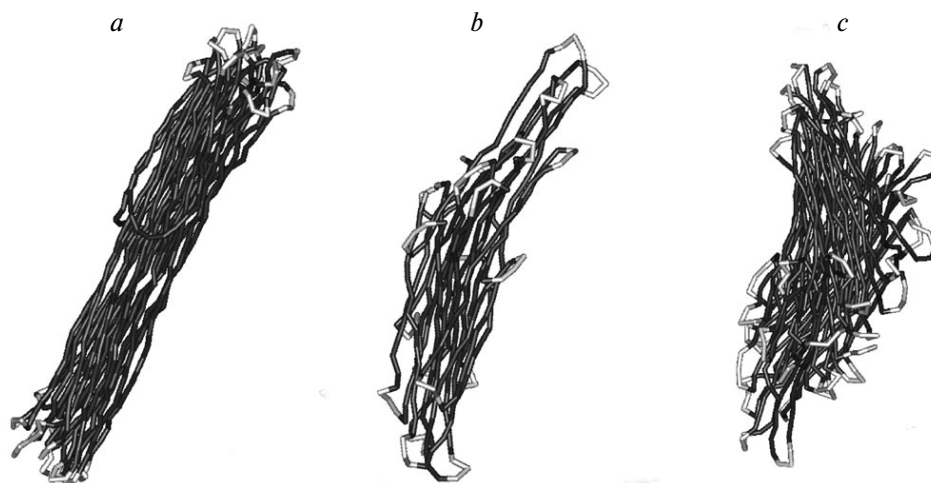


Fig. 7. Some typical examples for the final states of the collapsed chain of an *AB* copolymer (the chain is shown as a wire model) in the case of short junctions $n_f = 3$ between stiff blocks at $T = 1\epsilon/k_B$: $N = 378$, $n_s = 15$ (*a*); $N = 693$, $n_s = 30$ (*b*); $N = 756$, $n_s = 15$ (*c*). The conditions of a poor solvent are fulfilled for the stiff segments of a chain that are built of the type *A* beads.



Fig. 8. An example of the final states of the collapsed chain of a regular AB copolymer (the chain is shown as a wire model) at $T = 1\epsilon/k_B$ for $N = 1260$: $n_s = n_f = 9$ (a); 15 (b); and 30 (c). The conditions of a poor solvent are fulfilled for the flexible segments of a chain that are built of the type B beads.

the possibility of pore size control makes it possible to use such structures as a basis for design of novel porous materials, which can find application in catalytic and separation processes.

This work was financially supported by the Russian Foundation for Basic Research (Project No. 09-03-01183-a).

References

1. A. Yu. Grosberg, A. R. Khokhlov, *Statistical Physics of Macromolecules*, Aip Press, New York, 1994, 350 p.
2. M. Rubinstein, R. H. Colby, *Polymer Physics*, Oxford University Press, Oxford, 2003, 454 pp.
3. A. L. Lehninger, *Principles of Biochemistry*, N. Y. Worth Publ. Inc., New York, 1982, Vol. 1.
4. M. P. Taylor, *J. Chem. Phys.*, 2001, **114**, 6472.
5. M. P. Taylor, *J. Chem. Phys.*, 2003, **118**, 883.
6. M. R. Stukan, V. A. Ivanov, A. Yu. Grosberg, W. Paul, K. Binder, *J. Chem. Phys.*, 2003, **118**, 3392.
7. T. M. Birshtein, A. A. Merkur'eva, *Vysokomol. Soedin., Ser. A*, 1985, **27**, 1208 [*Polym. Sci. USSR, Ser. A*, 1985, **27**, 1201].
8. A. A. Sariban, T. M. Birshtein, A. M. Skvortsov, *Vysokomol. Soedin., Ser. A*, 1977, **19**, 2582 [*Polym. Sci. USSR, Ser. A*, 1977, **19**, 1728].
9. H. Noguchi, K. Yoshikawa, *J. Chem. Phys.*, 1998, **109**, 5070.
10. M. Baiesi, E. Carlon, E. Orlandini, A. L. Stella, *Phys. Rev. E: Stat. Phys. Plasmas*, 2001, **63**, 041801.
11. J. Ma, J. E. Straub, E. I. Shakhnovich, *J. Chem. Phys.*, 1995, **103**, 2615.
12. A. Montesi, M. Pasquali, F. C. MacKintosh, *Phys. Rev. E: Stat. Phys. Plasmas*, 2004, **69**, 21916.
13. B. Schnurr, F. C. MacKintosh, D. R. M. Williams, *Europhys. Lett.*, 2000, **51**, 279.
14. B. Schnurr, F. Gittes, F. C. MacKintosh, *Phys. Rev. E: Stat. Phys. Plasmas*, 2002, **65**, 061904.
15. E. Hernandez, I. R. Cooke, D. R. M. Williams, <http://arxiv.org/abs/cond-mat/0406558>.
16. V. V. Vasilevskaya, V. A. Markov, P. G. Khalatur, A. R. Khokhlov, *J. Chem. Phys.*, 2006, **124**, 144914.
17. J. A. Martemyanova, M. R. Stukan, V. A. Ivanov, W. Paul, K. Binder, *J. Chem. Phys.*, 2005, **122**, 174907.
18. M. R. Stukan, V. A. Ivanov, A. Yu. Grosberg, W. Paul, K. Binder, *J. Chem. Phys.*, 2003, **118**, 3392.
19. Y. Zhou, C. K. Hall, M. Kaplus, *Phys. Rev. Lett.*, 1996, **77**, 2822.
20. I. R. Cooke, D. R. M. Williams, *Macromolecules*, 2004, **37**, 5778.
21. Y. Zhou, M. Karplus, J. M. Wichert, C. K. Hall, *J. Chem. Phys.*, 1997, **107**, 10691.
22. W. Paul, M. Müller, *J. Chem. Phys.*, 2001, **115**, 630.
23. A. R. Khokhlov, P. G. Khalatur, *Curr. Opin. Solid State Mater. Sci.*, 2004, **8**, 3.
24. P. G. Khalatur, A. R. Khokhlov, *Adv. Polym. Sci.*, 2006, **195**, 1.
25. P. Flory, *Statistical Mechanics of Chain Molecules*, Wiley-Interscience, New York, 1969, 432 pp.
26. M. P. Allen, *Mol. Phys.*, 1980, **40**, 1073.
27. F. Guarnieri, W. C. Still, *J. Comput. Chem.*, 1994, **15**, 1302.
28. L. D. Landau, E. M. Lifshitz, *Statistical Physics*, Part 1, Vol. 5, Butterworth-Heinemann, 1980, 544 pp.
29. L. Verlet, *Phys. Rev.*, 1967, **159**, 98.
30. J. P. Ryckaert, C. Giovanni, H. J. C. Berendsen, *J. Comput. Phys.*, 1977, **23**, 327.
31. A. V. Dobrynin, M. Rubinstein, S. P. Obukhov, *Macromolecules*, 1996, **29**, 2974.
32. C. Holm, J. F. Joanny, K. Kremer, R. R. Netz, P. Reineker, C. Seidel, T. A. Vilgis, R. G. Winkler, *Adv. Polym. Sci.*, 2004, **166**, 67.
33. K. Yoshikawa, N. Yoshinaga, *J. Phys. Condens. Matter*, 2005, **17**, 2817.

Received March 12, 2010;
in revised form November 16, 2010